Available online at www.sciencedirect.com
SCIENCE DIRECT®
Remote Sensing of Environment 90 (2004) 86–103
Remote Sensing of Environment
www.elsevier.com/locate/rse

Detection limits of coral reef bleaching by satellite remote sensing: Simulation and data analysis

Hiroya Yamano*, Masayuki Tamura

Social and Environmental Systems Division, National Institute for Environmental Studies, 16-2 Onogawa, Tsukuba, Ibaraki 305-8506, Japan

Received 6 October 2003; received in revised form 26 November 2003; accepted 2 December 2003

Abstract

Monitoring of coral reef bleaching has hitherto been based on regional-scale, in situ data. Larger-scale trends, however, must be determined using satellite-based observations. Using both a radiative transfer simulation and an analysis of multitemporal Landsat TM images, the ability of satellite remote sensing to detect and monitor coral reef bleaching is examined. The radiative transfer simulation indicates that the blue and green bands of Landsat TM can detect bleaching if at least 23% of the coral surface in a pixel has been bleached, assuming a Landsat TM pixel with a resolution of 30×30 m on shallow (less than 3 m deep) reef flats at Ishigaki Island, Japan. Assuming an area with an initial coral coverage of 100% and in which all corals became completely bleached, the bleaching could be detected at a depth of up to 17 m. The difference in reflectance of shallow sand and corals is compared by examining multitemporal Landsat TM images at Ishigaki Island, after normalizing for variations in atmospheric conditions, incident light, water depth, and the sensor's reaction to the radiance received. After the normalization, a severe bleaching event when 25–55% of coral coverage was bleached was detected, but a slight bleaching event when 15% of coral coverage was bleached was not detected. The simulation and data analysis agreed well with each other, and identified reliable limits for satellite remote sensing for detecting coral reef bleaching. Sensitivity analysis on solar zenith angle, aerosol (visibility) and water quality (Chl *a* concentration) quantified the effect of these factors on bleaching detection, and thus served as general guidelines for detecting coral reef bleaching. Spatial misregistration resulted in a high degree of uncertainty in the detection of changes at the edges of coral patches mainly because of the low (~30 m) spatial resolution of Landsat TM, indicating that detection of coral reef bleaching by Landsat TM is limited to extremely severe cases on a large homogeneous coral patch and shallow water depths. Satellite remote sensing of coral reef bleaching should be encouraged, however, because the development and deployment of advanced satellite sensors with high spatial resolution continue to progress.

Keywords: Coral reef; Bleaching; Radiative transfer model; Landsat TM; Ishigaki Island

1. Introduction

Coral reef bleaching is a major scientific and environmental issue (Brown, 1997; Glynn, 1993). Bleaching frequency has increased since the early 1980s, and a severe global bleaching event took place in 1997 and 1998 (Wilkinson, 2000). One possible reason for the increased frequency of bleaching might be related to high sea-surface temperatures (SST) caused by global warming (Hoegh-Guldberg, 1999).

The loss in pigmented zooxanthellae from corals during bleaching events results in an optical signal that is strong enough for remote sensing to detect. Although global SST is monitored by the NOAA AVHRR sensor (Goreau & Hayes, 1994; Strong et al., 1997), studies on coral bleaching are based on in situ data (e.g., Holden & LeDrew, 1998; Myers et al., 1999), kite photography (Hasegawa et al., 1999), and aerial photography (Andréfouët et al., 2002) at a relatively small spatial scale. Satellite remote sensing should be investigated, because satellite sensors can routinely obtain data on coral reefs on a large spatial scale of ca. 100×100 km.

To examine the applicability of satellite remote sensing to coral reef assessment, the detection limits must be constrained. Because coral reefs are highly heterogeneous, the spatial resolution of currently available, widely used satellite imagery (e.g., Landsat TM, Landsat ETM+) is considered to be too coarse to map reefs in detail (Andréfouët et al., 2001;

* Corresponding author. Fax: +81-29-850-2572.
E-mail address: hyamano@nies.go.jp (H. Yamano).

0034-4257/$ - see front matter © 2004 Elsevier Inc. All rights reserved.
doi:10.1016/j.rse.2003.12.005

Mumby et al., 1998b). Most coral reef bleaching studies have suggested that it is difficult for satellite sensors to detect coral bleaching, mainly because of the sensors' low (~30 m) spatial resolution relative to the scale of reef heterogeneity (e.g., Holden & LeDrew, 1998). Study of aerial photographs taken during the 1998 bleaching event shows that information on bleached corals can be obtained only by sensors with high (<2 m) spatial resolution (Andréfouët et al., 2002). A further complication is that analysis of a single image might not correctly identify pixels that contain both healthy and bleached corals, because pixels that contain other substrate features, such as sand, can have reflectance characteristics similar to those of pixels showing partially bleached corals. Comparison of multitemporal images allows more accurate assessment of the detection limits for bleached corals in a pixel, because an increase in reflectance will be recorded where bleaching has taken place.

This study shows the detection limits of coral reef bleaching events by satellite remote sensing. Landsat TM was selected as one of the most effective satellite sensors, because it has higher spatial resolution (30 m) than global sensors such as NOAA AVHRR (1 km) or Terra MODIS (250 m to 1 km), which would contribute to a better mapping of coral reefs with high heterogeneity. It has an observation band for blue and green light that penetrates water well, and has been widely used for coral-reef mapping and monitoring (e.g., Ahmad & Neil, 1994; Matsunaga et al., 2000). Landsat TM has been used for data acquisition on coral reefs since 1984, and could be useful in interpreting coral reef dynamics over the past 20 years. Moreover, continuity of TM imagery in the future is ensured by the launch of Landsat 7 with the ETM+ sensor (Andréfouët et al., 2001). Further advantage of Landsat TM was shown by Mumby and Edwards (2002) that Landsat TM was most cost-effective sensors for mapping coral reefs in the viewpoint of price and mapping accuracy. Finally, the similar wavebands are assigned for high spatial resolution sensors such as IKONOS and QuickBird, and so the results obtained for Landsat TM should be applicable to those recent high-resolution sensors.

In this paper, two approaches are used to examine the feasibility of using Landsat TM to detect coral bleaching. One approach is based on radiative transfer simulation, and the other is based on multitemporal satellite data analysis. The simulation results are compared with the results of satellite data analysis, which are validated by comparison with in situ data; together, these two approaches delineate the conditions under which satellite remote sensing can be used to assess coral reef bleaching.

Simulating the radiance received by a satellite sensor is very effective in assessing the feasibility of satellite remote sensing in done properly. Lubin et al. (2001) calculated the radiance received by satellites using a coupled ocean-atmosphere radiative transfer model, and showed that from space, most corals are distinguishable from brighter non-coral objects such as sand. Andréfouët et al. (2001) simulated the DN (digital number) received by Landsat ETM+ sensors and showed that the Landsat ETM+ could detect changes in three ubiquitous substrate classes: sand, background (rubble, pavement, and heavily grazed dead corals), and foreground (living corals and macroalgae). Yamano and Tamura (2002) calculated the radiance received by Landsat TM from healthy and bleached corals to examine the utility of Landsat TM in detecting coral reef bleaching, using reflectance data from a previous study (Holden & LeDrew, 1998). The simulation of Yamano and Tamura (2002) was updated using coral reflectance spectra obtained in the Ryukyu Islands (Yamano et al., 2002) during a bleaching event that occurred in the summer of 2001 (Strong et al., 2002).

In analyzing multitemporal satellite data, it is critical to remove or normalize the effects of changes in atmosphere, incident light, water depth, and sensor response (e.g., Mumby et al., 1998a; Thome et al., 1997). To remove the effects of path radiance and reflectance at the sea surface, an offset between deep-water and shallow-water radiance has been widely used (e.g., Lyzenga, 1978, 1981; Mumby et al., 1998a,b). The effect of water depth can be removed by calculating depth-invariant indices of bottom type (Lyzenga, 1981). This method calculates the ratio of attenuation coefficients between two bands of satellite sensors based on a scatter plot of log-transformed DN values of the bands, and thus is less sensitive to change in DN values. This reduced sensitivity is disadvantageous for detecting coral reef bleaching. DN or radiance values of multitemporal images must be compared directly. Satellite images commonly include clouds, which can mimic variations in atmospheric effects from site to site within an image. Clouds may also affect incident light on a nearby site. A new method to normalize these effects is used (Yamano & Tamura, 2001) to reveal the changes in DN values of corals from 1984 to 2000.

2. Methods

2.1. Study area and validation sites

The distribution of corals and algae on Ishigaki Island, southwestern Japan (Fig. 1) have been intensively surveyed, and a detailed map of coral distribution (*Acropora*, *Montipora* and *Porites*), algae and seagrass has been published by the Environment Agency (1996) based on surveys taken from 1989 to 1992. In some reefs, the proportion of healthy coral cover prior to the summer of 1998 exceeded 50% of the substrate (Environment Agency, 1996). The global-scale mass-bleaching event of 1997–1998 (Wilkinson, 2000) caused a significant loss of healthy corals in Japan's reefs (e.g., Kayanne et al., 2002). Hasegawa et al. (1999) showed that bleaching began between 20 June and 10 August 1998. From 10 August to 10 September, severe bleaching was observed in many reefs due to high SST. The status of corals

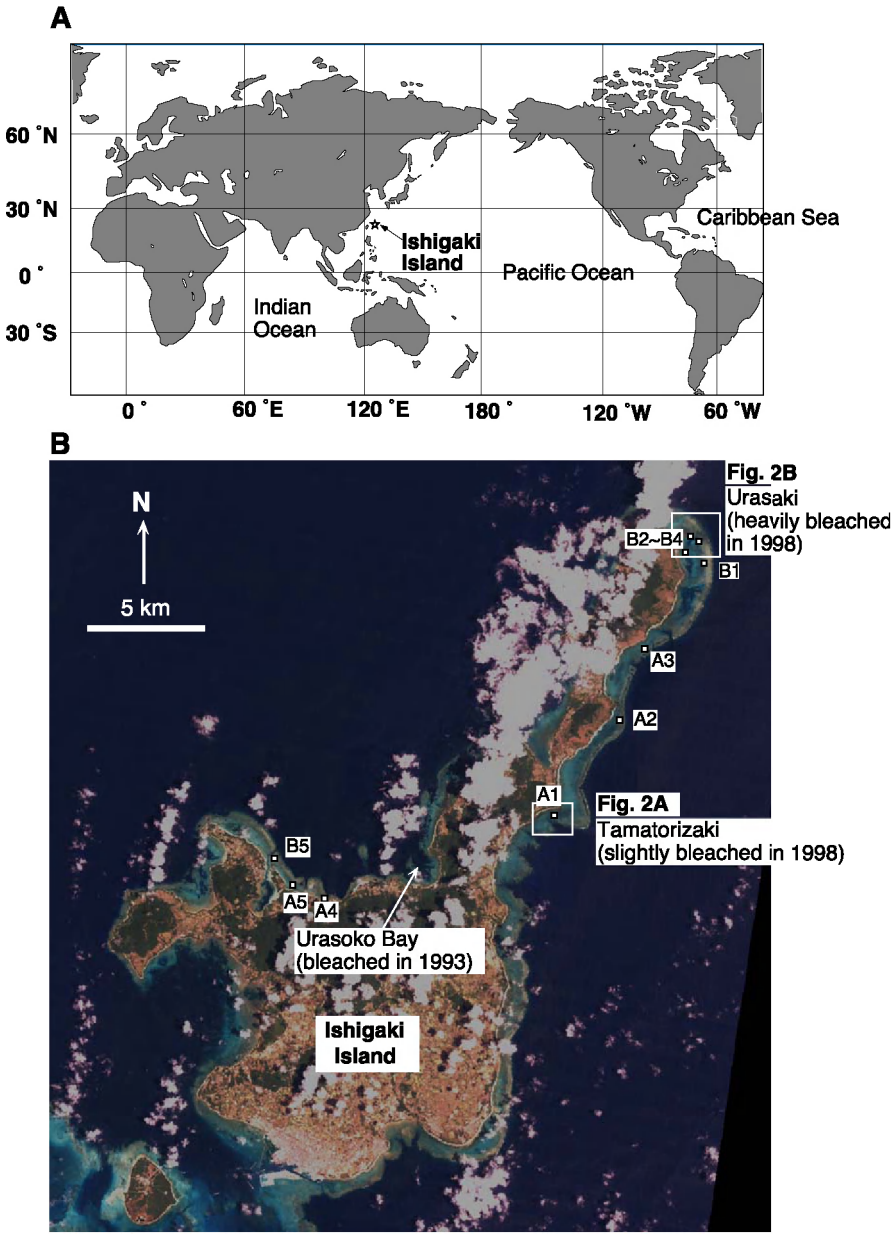

Fig. 1. (A) Location of Ishigaki Island, in the Ryukyu Islands, Japan. (B) Landsat TM image of Ishigaki Island obtained on 15 August 1998, when the severe bleaching event occurred, and validation sites (Table 1). Note many clouds over and around the island. Locations of Tamatorizaki and Urasaki reefs are indicated.

before and just after the bleaching around Ishigaki Island was monitored at 72 sites by the Environment Agency of Japan (Environment Agency, 1999). After the 1998 bleaching, the status of corals at the same sites has been monitored continuously once a year (Environment Agency, 2000a,b). The location of these sites was determined by a GPS with an accuracy of ca. ±10 m. At every site, two surveyors visually investigated the coral coverage within an area of ca. 50×50 m (Yoshida, personal communication). Thus, the data can be compared with that of Landsat TM whose spatial resolution is 30×30 m. Prior to 1998, the most significant bleaching event reported for Ishigaki Island was in the summer of 1993, when approximately 55% of corals were reported to have been bleached at Urasoko Bay (Fig. 1; Fujioka, 1999), although no information was provided at other sites. The existence and timing of bleaching events prior to 1990 are unknown. In summer 2001, a coral bleaching event took place in the Ryukyu Islands as a result of high SST (Strong et al., 2002). In this bleaching event, however, the proportion of dead corals was comparatively small.

In order to validate the results of satellite data analysis, we used data provided by the Environment Agency (1999) and Hasegawa et al. (1999). Unfortunately, the Landsat TM image for August 15, 1998, which should have recorded the coral reef bleaching event, contained many clouds that covered most of Ishigaki Island and adjacent reefs (Fig.

1). Thus, the number of sites for validation is limited. Furthermore, because satellite-based pixel-level change detection has high sensitivity to spatial misregistration while georeferencing the images (Stow, 1999), it is recommended that only points situated within large coral patches (>90×90 m) should be used after all of the images were georeferenced with rms errors smaller than 1.0 (see Satellite data analysis). Since changes in river water discharge could significantly affect the water quality, sites near a river month were excluded. Furthermore, sites facing directly toward open oceans (e.g., reef edge) should be excluded, because foam and whitecaps due to breaking waves contribute to a portion of the radiance in those locations. As a result, we were limited to the use of only nine points out of 72 surveyed by the Environment Agency (1999) and one point (B3) out of five surveyed by Hasegawa et al. (1999) for validating satellite-based time-series change analysis (Table 1). These sites were classified into two categories according to the percent cover of bleached corals: slightly or non bleached sites showed less than 15% cover of bleached corals, while heavily bleached sites showed more than 25% cover of bleached corals (Table 1). In the severely bleached sites, the bleached corals died, and the sites were latter occupied by dead coral rubble, which was observed by one of the authors (H.Y.) in March 2001. Furthermore, we selected two reefs (Urasaki and Tamatorizaki) as being representative of severely bleached and slightly bleached areas, respectively (Figs. 1 and 2, Table 1), to investigate the potential area of bleaching (see Satellite data analysis).

2.2. Radiative transfer simulation

The reflectance from bleached and healthy corals was simulated in order to examine the feasibility of using Landsat TM to detect coral reef bleaching. Fig. 3 shows the components of radiance received by a satellite sensor. It is the difference between the radiance from a pixel containing healthy corals before a bleaching event and the radiance from the same pixel after the event that is of interest. Radiance was calculated by entering the healthy and bleached coral reflectance spectra obtained by Yamano et al. (2002) (Fig. 4) who measured the reflectance in a flume with black fabric to minimize wall effects in the light field. The reflectance spectra were measured 10 cm above the reference panel and above the corals. The reflectance of healthy corals showed values similar to those of common brown-colored corals previously reported (Hochberg & Atkinson, 2000; Hochberg et al., 2003; Holden & LeDrew, 1998), as supported by Holden and LeDrew (1999) who showed that geographic location did not affect the spectral reflectance characteristics of healthy corals. In contrast, the reflectance of bleached corals was significantly higher than previously reported (Hochberg et al., 2003; Holden & LeDrew, 1998; Myers et al., 1999). Of greatest importance is the absence of absorption in the red region, which indicates the loss of zooxanthellae. The bleached coral measured here still contained 1.1×10^4 healthy zooxanthellae per cm^2, but this number was 1/100 of the number of the healthy coral measured (Yamano et al., 2003). The bleached coral is regarded here as a still-living coral that has lost

Table 1
Status of corals before and after the 1998 bleaching event (Environment Agency 1999, 2000a,b; Hasegawa et al., 1999)

Site ID	Location	Latitude	Longitude	Depth [m]	Bleached coral coverage in 1998 summer [%]	Corals	Healthy coral coverage [%]			
							Before the 1998 bleaching	September to November 1998	October to November 1999	August to October 2000
Slightly or non bleached sites										
A1	Tamatorizaki	24:29:07.6	124:16:40.7	1.5–2.5	15	Branching *Porites*	70	55	50	55
A2	Tomuruzaki	24:31:31.6	124:18:32.2	1.0–2.5	5	Branching *Montipora*	10	5	5	5
A3	Yasurazaki	24:33:15.6	124:19:11.2	1.0–3.0	10	Various corals	30	20	5	10
A4	Kabira	24:27:05.4	124:10:07.1	1.0–2.0	0	Massive *Porites*	10	10	10	10
A5	Kabira	24:27:25.6	124:09:18.9	1.0–3.0	5	Branching *Acropora*, Branching *Montipora*	10	5	5	10
Severely bleached sites										
B1	Urasaki	24:35:33.6	124:20:55.1	1.0–3.0	55	Branching *Acropora*	60	5	10	10
B2	Urasaki	24:36:14.2	124:20:45.0	1.0–5.0	45	Branching *Montipora*	50	5	10	15
B3	Urasaki	24:35:52	124:20:24.17	1.0–2.0	>50	Branching *Montipora*	>50	0	N/A	N/A
B4	Urasaki	24:36:14.8	124:20:31.7	1.0–2.0	50	Encrusting/Branching *Montipora*, Branching *Acropora*	60	10	10	10
B5	Kabira	24:28:07.6	124:08:50.2	0.5–1.5	25	Branching *Acropora*	40	15	10	10

Site IDs as in Fig. 1.
Original data for coral coverage (Environment Agency 1999, 2000a,b) was based on the percentage of healthy corals to consolidated substrates, and it was converted to percentage of healthy corals to all the substrates according to Yoshida (personal communication).

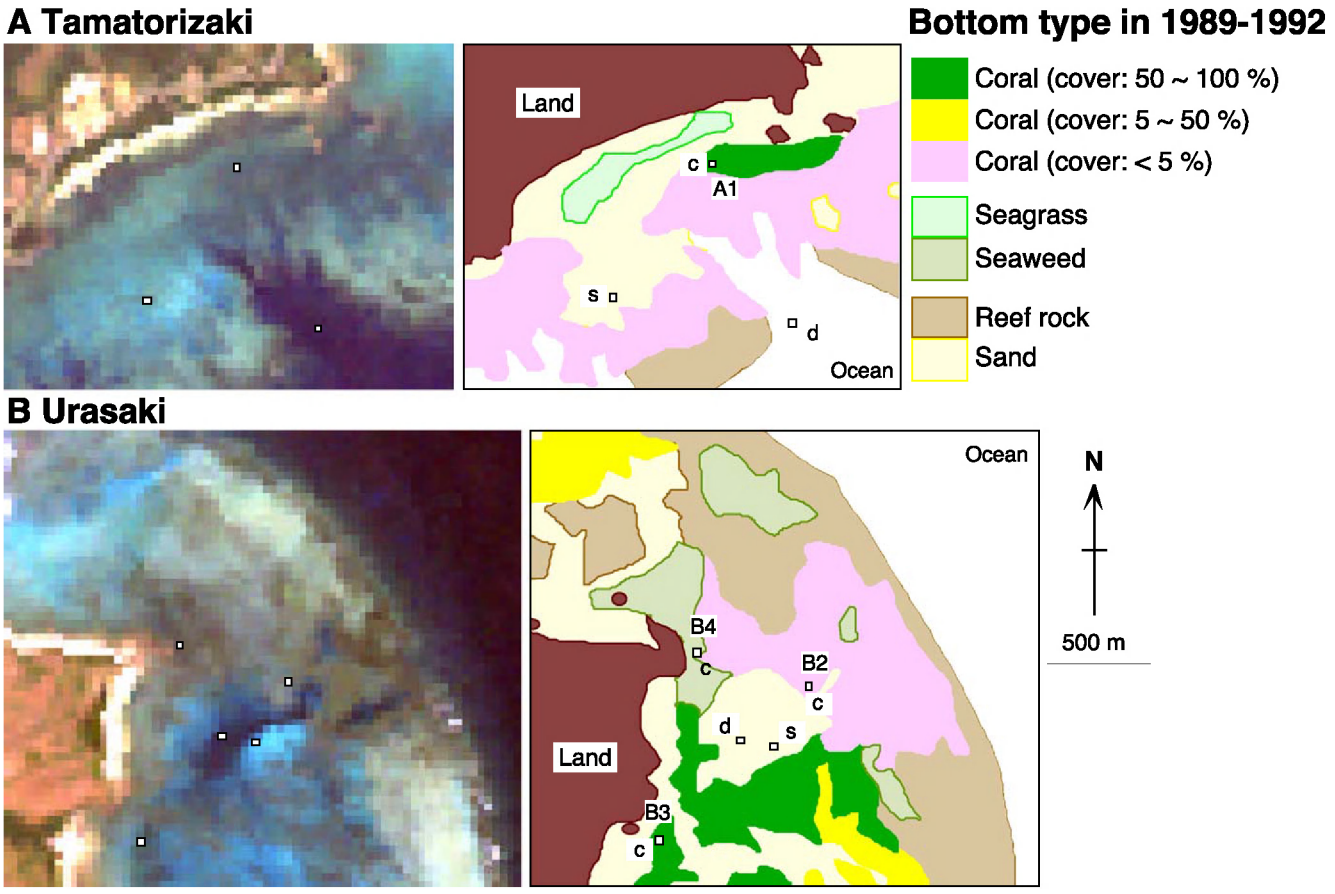

Fig. 2. Landsat TM image (15 August 1998) of (A) Tamatorizaki and (B) Urasaki reefs and bottom types in 1989–1992 (Environment Agency, 1996). *S*, *d* and *c* show points occupied by sand, deep water, and corals, whose DN values were used for analysis.

almost all of its symbionts, while the bleached corals shown by Holden and Ledrew (1998) could be regarded in a progressive phase of bleaching, because the reflectance shows absorption feature by chlorophyll (Fig. 4). The data of Yamano et al. (2002) show the maximum reflectance of bleached coral, and so are useful for examining the satellite remote sensing detection limits for bleached coral.

The simulation procedure was based on that of Yamano and Tamura (2002). We calculated the radiance at Landsat TM bands 1, 2 and 3 in the visible region. Two radiative transfer models for calculating radiance were used: 6S (Vermote et al., 1997) and Hydrolight (Mobley, 1994). 6S was used for calculating photon absorption and scattering in the atmosphere. Hydrolight was used for calculating reflectance at the sea surface and photon absorption and scattering in seawater. Hydrolight computes spectral radiance both within water bodies and as the radiance leaves water bodies, based on the invariant imbedding theory. The calculated radiance from the sand substratum agreed well with that recorded by Landsat TM, validating the use of these two models in a coral-reef environment (Yamano & Tamura, 2002).

We calculated the radiance from bleached and healthy corals in order to examine the feasibility of using Landsat TM to detect coral reef bleaching. The basic parameters were prepared for the validation site, Ishigaki Island (Table 2). We calculated the path radiance (L_a in Fig. 2), transmittance of the air, and incident light at the sea surface using 6S. Atmospheric condition was set to tropical type with a visibility of 40 km, and solar zenith angle was set to 25°, considering the early- to mid-summer conditions at Ishigaki Island. Then, using Hydrolight, we calculated the radiance reflected from sea surface (L_r) and the radiance from the bottom features (L_w) by input of the values of incident light calculated by 6S. Wind speed was set to 0 m s^{-1}, as the wind has little effect on the irradiance reflectance at sea surface in the absence of foam and whitecaps for small solar zenith angles (e.g., Bukata et al., 1995). Winds at the image acquisition time (Table 3) were less than 5 m s^{-1}. We set chlorophyll a (Chl *a*) concentration to 0.5 mg m^{-3}, because the Chl *a* value range from 0.1 to 0.8 mg m^{-3} in the backreef lagoon of Ishigaki Island (Hata, personal communication). The scattering and absorption in the seawater volume were calculated according to Haltrin (1999). The radiance leaving the water was then multiplied by the direct transmittance of the air calculated by 6S, and the radiance (W m^{-2} sr^{-1} μm^{-1}) from the pixel of interest received by Landsat TM was obtained. We calculated the difference of

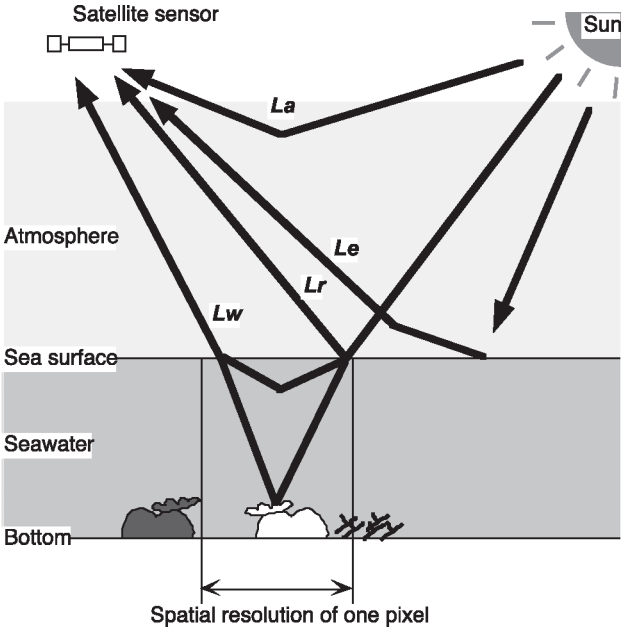

Fig. 3. Components of the radiance received by a satellite sensor for one pixel and the terminology used to identify them in this study. L_w, the water-leaving radiance from the substrate at the bottom of the water column and from the radiance scattered by water molecules and microscopic particles; L_r, the radiance reflected from the sea surface; L_e, the radiance from adjacent pixels; and L_a, the path radiance (radiance scattered by the atmosphere).

the radiance before and after a bleaching event as a function of water depth and the difference in healthy coral coverage before and after the bleaching event.

In order to apply our result to bleaching detection in other regions and assess the impact of other parameters (solar zenith angle, visibility, and Chl *a* concentration), additional calculations were made for three combinations of: solar zenith angle (0–50°) and water depth (0.1–30 m), visibility (5–100 km) and water depth, and Chl *a* concentration (0.01–2.0 mg m^{-3}) and water depth, assuming an area with an initial coral coverage of 100% and in which all corals became completely bleached. Other parameters were set to the same as those shown in Table 2.

The noise amplitudes (DN values) of TM bands 1, 2, and 3, which are critical for change detection, was estimated to be 2, 1, and 1 (standard deviations), respectively, based on the fluctuation of deep ocean values (Yamano & Tamura, 2002). The difference in DN values needed to detect coral bleaching is assumed to be twice these values, or 4, 2 and 2, for bands 1, 2 and 3, respectively. Thus, the difference in radiance values calculated using Thome et al. (1997) coefficients are 3.27, 3.06, and 2.25 W m^{-2} sr^{-1} μm^{-1}, respectively.

2.3. Satellite data analysis

Landsat 5 TM images (PATH 115, ROW 43) obtained from 1984 to 2000 were analyzed (Table 3). These data include the image of 15 August 1998 (Fig. 1), when the severe bleaching event occurred. All of the images were georeferenced with rms errors smaller than 1.0. Only summer images were used, because bleaching is generally caused by the high SST under strong incident light from the higher solar elevation angles. In addition, the abundance of seaweed, whose reflectance spectra are similar to those of healthy coral, shows significant seasonal changes (e.g., Lirman & Biber, 2000), a phenomenon that is also observed at Ishigaki Island (Akatsuka, 2001). These characteristics would disturb the detection of coral reef bleaching in multitemporal data taken in different seasons.

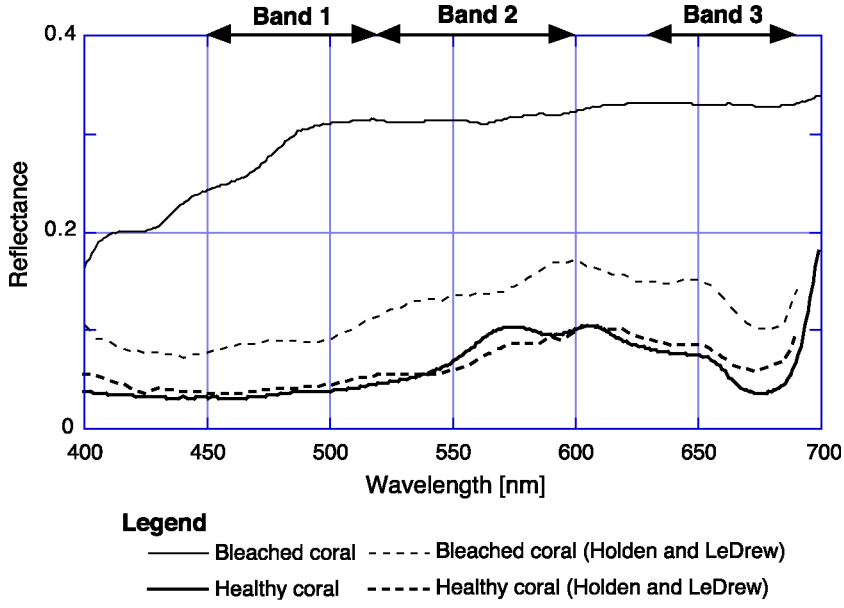

Fig. 4. Reflectance spectra of healthy and bleached *Montipora digitata* measured in a flume with black fabric. Data of Holden and LeDrew (1998) are also shown. The widths of Landsat TM bands 1–3 are indicated in the upper part of the figure.

Table 2
Basic parameters used in the radiative transfer models

Sensor conditions	
Sensor type	Landsat TM Bands 1–3
Sun zenith angle	25°
Sensor zenith angle	0°
Atmospheric conditions for 6S	
Atmosphere type	Tropical
Aerosol type	Maritime
Visibility	40 km
Surface conditions for Hydrolight	
Altitude	0 m
Wind speed	0 m s^{-1}
Seawater condition for Hydrolight	
Seawater type	Case I
Variables for Hydrolight	
Water depth	0.1–30 m
Chlorophyll concentration	0.5 mg m^{-3}
Bottom type	Healthy coral, Bleached coral

We compared the DN from each pixel in the multitemporal images after removing the effects of path radiance, radiance from adjacent pixels, and the reflectance of seawater (Fig. 3), and then normalizing the effects of changes in the atmosphere, incident light, water depth and sensor response. In this comparison, four assumptions were made: (1) the atmosphere is spatially uniform over a reef within a single image; (2) the incident light on the reef of interest is spatially uniform within an image; (3) the water quality (extinction coefficient) over the reef of interest is the same in any two images; and (4) the reflectance of sand and deep water are constant in any two images. This normalization method was originally proposed by Yamano and Tamura (2001) and is described in detail here. It does not require knowledge of differing atmospheric conditions or water depths due to tide among the images, both of which have been problematic in previous attempts to monitor coral reefs by satellite (Lyzenga, 1978; Mumby et al., 1998a). To properly normalize each scene DN values from three types of substrate——shallow sand (DN_s), deep water (DN_d), and corals (DN_c)——are needed. These points should be as close as possible to each other spatially (Fig. 2) in order to reduce the possibility of local changes in atmospheric conditions and incident light due to the presence of clouds near the site (Fig. 1). Furthermore, radiance from adjacent pixels (L_e in Fig. 3) is assumed to be the same for the three pixels, because the pixels are close to each other. The basic procedure is to compare the differences in DN values between sand (DN_s) and corals (DN_c) in multitemporal satellite images, after normalizing for changes in the atmosphere (transmittance), incident light, sensor characteristics, and water depth. If the value of (DN_s—DN_c) in one image is smaller than in other images, coral bleaching would be interpreted to have taken place, because DN_s should be constant and the DN_c value of bleached corals should be greater than that of healthy corals.

The digital number (DN_t) generated by a satellite sensor (Fig. 3) is a function of the radiance received at the sensor and is given for an individual pixel by

$$DN_t = G[L_w + L_r + L_e + L_a] + B \quad (1)$$

where G and B are the gain and offset values for converting the radiance to DN. In our work, the effect of multiple scattering in air and in seawater was ignored.

Table 3
Collected landsat TM images

Image acquisition date	Water level [cm]	Slightly or non bleached sites					Severely bleached sites					Remarks
		A1	A2	A3	A4	A5	B1	B2	B3	B4	B5	
1984.8.24	45			*	*	*			#	#	*	
1985.7.10	130		*	*	*	*	*				*	
1987.8.17	105	*	*	*	*	*					*	
1988.7.18	165	*	*	*	*	*	*	*	*	*	*	
1989.7.5	140	*	*	*	*	*	*	*	*	*	*	
1990.7.24	150				*	*	*	*	*	*	*	
1991.7.11	60	*		*	*	*		*	*	*	*	
1993.6.30	50	*	*	*	*	*			#	#	*	Possible bleaching
1994.5.16	160											Reference
1994.9.5	80	*		*							#	
1995.8.7	50			*	*	*	*		#	#	*	
1996.7.8	125	*	*				*	*	*	*		
1997.7.27	130	*					*					
1998.6.28	175				*	*					*	Beginning of bleaching
1998.8.15	125											Bleaching
2000.7.19	140	*			*	*					*	

Asterisks (*) indicate the existence of clouds at the site, and the data was not be used.
Sharps (#) indicate the possible subaerial exposure of the site due to low tide, and the data was not be used.
The image in May 1994 was used for reference.

Radiance from the substrate is described as follows:

$$L_w = T\mathrm{Ed}C\rho_b\exp[-2kz] \quad (2)$$

where T is light transmittance in air, Ed is downwelling irradiance above the sea surface within the given spectral band and the time of year and day when the image was collected, C is a factor that accounts for the loss of irradiance at the air–sea interface due to reflectance (e.g., Kirk, 1994), ρ_b is the reflectance of bottom features, k is an extinction coefficient for water, and z is the water depth.

Consider the DN values from sand, deep water, and coral (DN_s, DN_d, and DN_c) in two images collected on different dates (images 1 and 2). Based on Eqs. (1) and (2), in the first image, the DN values are given by

$$DN_{s1} = G_1[L_{s1} + L_{r1} + L_{e1} + L_{a1}] + B_1 \quad (3)$$

$$DN_{d1} = G_1[L_{d1} + L_{r1} + L_{e1} + L_{a1}] + B_1 \quad (4)$$

$$DN_{c1} = G_1[L_{c1} + L_{r1} + L_{e1} + L_{a1}] + B_1 \quad (5)$$

where

$$L_{s1} = T_1\mathrm{Ed}_1C_1\rho_{s1}\exp[-2k_1z_{s1}] \quad (6)$$

$$L_{d1} = T_1\mathrm{Ed}_1C_1\rho_{d1}\exp[-2k_1z_{d1}] \quad (7)$$

$$L_{c1} = T_1\mathrm{Ed}_1C_1\rho_{c1}\exp[-2k_1z_{c1}] \quad (8)$$

In the second image, in which the water depth exceeds that of the first image by Δz due to tide, the DN values are given by

$$DN_{s2} = G_2[L_{s2} + L_{r2} + L_{e2} + L_{a2}] + B_2 \quad (9)$$

$$DN_{d2} = G_2[L_{d2} + L_{r2} + L_{e2} + L_{a2}] + B_2 \quad (10)$$

$$DN_{c2} = G_2[L_{c2} + L_{r2} + L_{e2} + L_{a2}] + B_2 \quad (11)$$

where

$$L_{s2} = T_2\mathrm{Ed}_2C_2\rho_{s2}\exp[-2k_2(z_{s1} + \Delta z)] \quad (12)$$

$$L_{d2} = T_2\mathrm{Ed}_2C_2\rho_{d2}\exp[-2k_2(z_{d1} + \Delta z)] \quad (13)$$

$$L_{c2} = T_2\mathrm{Ed}_2C_2\rho_{c2}\exp[-2k_2(z_{c1} + \Delta z)] \quad (14)$$

Here, $\rho_{s1}=\rho_{s2}=\rho_s$, $\rho_{d1}=\rho_{d2}=\rho_d$, and $k_1=k_2=k$, according to the assumptions described above.

The effects of adjacent pixels, path radiance, and the offset in converting the radiance to DN are removed by subtracting DN_c from DN_s in the same image.

$$DN_{s1} - DN_{c1} = G_1T_1\mathrm{Ed}_1C_1[\rho_s\exp(-2kz_{s1}) - \rho_{c1}\exp(-2kz_{c1})] \quad (15)$$

$$DN_{s2} - DN_{c2} = G_2T_2\mathrm{Ed}_2C_2[\rho_s\exp(-2kz_{s1}) - \rho_{c2}\exp(-2kz_{c1})]\exp[-2k\Delta z] \quad (16)$$

In order to perform the normalization between the images, $(DN_{s1}-DN_{d1})$ should be made to be equal to $(DN_{s2}-DN_{d2})$ by introducing a coefficient α:

$$\alpha = \frac{DN_{s1} - DN_{d1}}{DN_{s2} - DN_{d2}} = \frac{G_1T_1\mathrm{Ed}_1C_1}{G_2T_2\mathrm{Ed}_2C_2\exp[-2k\Delta z]} \quad (17)$$

Thus, (DN_s-DN_c) in the second image (Eq. (16)) is normalized with respect to the first image using α:

$$\alpha[DN_{s2} - DN_{c2}] = G_1T_1\mathrm{Ed}_1C_1[\rho_s\exp(-2kz_{s1}) - \rho_{c2}\exp(-2kz_{c1})] \quad (18)$$

It can then be compared to Eq. (15) without knowledge of the atmospheric conditions or the difference in water depths due to tide between the two images, because the change in the DN value is produced only by the difference in coral reflectance (ρ_c).

The normalized values of (DN_s-DN_c) for Landsat TM bands 1–3 at 10 points (Table 2) in each image (Table 3) were compared with reference values of (DN_s-DN_d) from an image without clouds obtained on 16 May 1994, and the values were converted to radiance (W m^{-2} sr^{-1} μm^{-1}) using Thome et al. (1997) calibration coefficient for 1994. The propagation of errors due to Landsat TM sensor noise in the normalizing procedure was calculated. The calculated error magnitude was then used to estimate the detection limit for bleaching in the results of the radiative transfer simulation and the time-series satellite data analysis.

In addition to the time-series change analysis at ten points (Fig. 1; Table 1) the potential area of coral reef bleaching was extracted in two reefs (Urasaki and Tamatorizaki) which showed significantly different proportions of bleached corals (Figs. 1 and 2; Table 1). The potentially bleached areas were extracted by comparing the DN values of bands 1 and 2 between August 1995 and August 1998 (Tamatorizaki Reef) and between July 1997 and August 1998 (Urasaki Reef). Considering the errors produced in the normalizing procedure for both bands 1 and 2, pixels were extracted if the difference of radiance between the two images was greater than the sum of the resultant errors calculated for the two images.

3. Results and discussion

3.1. Radiative transfer simulation

3.1.1. Detection limits calculated for Ishigaki Island

Because the reflectance of bleached corals showed higher values in this study than the values of Holden and LeDrew (1998), which were used in the previous simulation by Yamano and Tamura (2002) (Fig. 4), the likelihood of detecting coral bleaching by Landsat TM could be greater previously shown. Fig. 5 shows the difference in DN values before and after a bleaching event as a function of water depth and the percentage of bleached corals in a TM pixel, which shows the difference in healthy coral coverage before and after the bleaching event. The detection limit of coral bleaching can be determined using Fig. 5. As described in the Methods section, it was assumed that coral bleaching could be detected if the difference in DN values was in excess of twice the error magnitude due to Landsat TM sensor noise. If a severe bleaching event occurred in an area that initially had an abundance of healthy corals (an area with an initial coral coverage of 100%, but in which all corals became completely bleached), the maximum detectable depths were 28, 21, and 3.0 m for bands 1, 2 and 3, respectively. The vertical lines in Fig. 5 indicate a depth of 3 m, which indicates the maximum depth of reef flats in general. If the DN values from a coral pixel between two images can be compared directly, then Landsat TM bands 1, 2 and 3 can detect, at a depth of 3 m, differences of 10%, 9% and 94%, respectively, in healthy coral coverage in a pixel on reef flats due to bleaching.

In analyzing satellite data, error propagation in the normalization procedure must be taken into consideration. The errors for Landsat TM bands 1, 2 and 3 after the normalization procedure ranged from 1.72 to 3.35, from 1.67 to 2.53, and from 0.56 to 2.18 in radiance (W m^{-2} sr^{-1} μm^{-1}), respectively. Thus, the difference in DN values used for bleaching detection should be 6.70, 5.06 and 4.36 for the respective bands, and we use these values hereafter for bleaching detection. Thus, if a severe bleaching event occurred in an area that initially had an abundance of healthy corals, the maximum detectable depths were 18, 17 and 1.7 m for bands 1, 2 and 3, respectively. On reef flats, a 23% difference and a 16% difference in healthy coral coverage in a pixel due to bleaching would be detected at a depth of 3 m using bands 1 and 2, respectively, of the Landsat TM (Fig. 5). Using band 3, the detection is limited to a shallow (1–2 m) part of the reef flat.

3.1.2. Effect of solar zenith angle, aerosol, and Chl a concentration on bleaching detection

The effect of solar zenith angle is indicated in Fig. 6A, which shows the difference in radiance values before and after a bleaching event as a function of solar zenith angle and water depth, assuming an area with an initial coral coverage of 100% and in which all corals became completely bleached. The maximum detectable depths were correlated well with sine value of solar zenith angle for all three bands, e.g., in band 1, they were 20, 18, and 11 m, for solar zenith angle of 0°, 25° and 50°, respectively. In low latitude area where solar zenith angle in summer is less than 25°, the effect of solar zenith angle should be small.

The effect of aerosol (visibility) is indicated in Fig. 6B. In all three bands, the significant effect of aerosol is observed in a condition of visibility smaller than ~25 km, while the effect is small in a condition of visibility greater than ~25 km. Under the condition of 5 km visibility, the maximum detectable depth was approximately half times as small as that of 40 km visibility.

The effect of Chl *a* depends on wavelength (band) (Fig. 6C). The greatest sensitivity of bleaching detection is observed in band 1. The maximum detectable depth increased significantly when Chl *a* concentration is below 0.8 mg m^{-3}, and exceeded 30 m when Chl *a* was smaller than 0.27 mg m^{-3}. On the other hand, in band 2, the detectable maximum depths were 24, 17 and 9 m, for Chl *a* of 0.01, 0.5 and 2.0 mg m^{-3}, respectively. In band 3, Chl *a* had little effect.

3.2. Satellite data analysis

Fig. 7 shows the temporal changes of differences in radiance values between sand and corals at 10 validation sites after applying the normalization procedure. The difference values at slightly or non bleached sites were almost stable for 17 years (from 1984 to 2000; Fig. 7A). Landsat TM could not detect less than 15% bleached coral cover in a pixel (Table 1) that developed during the 1998 bleaching event. It is our contention that the stability of the difference values in Fig. 7A demonstrates the effectiveness of the method used in this study, because the percentage of bleached corals at these sites was small even in 1998 (Environment Agency, 1999) and are considered to have remained small. On the other hand, the values of bands 1 and 2 at severely bleached sites were smallest in the summer of 1998 (Fig. 7B). This corresponds to the severe bleaching event at the sites (Table 1). The 1998 mass-bleaching event that produced 25–55% bleached coral cover would be detected by bands 1 and 2, as indicated by the radiative transfer simulation (Fig. 5). After 1997, the values of bands 1 and 2 decreased in June 1998 and reached their lowest values in August 1998, reflecting the progress of bleaching. This is supported by the fact that reflectance value of bleached corals shown by Holden and LeDrew (1998), which could be regarded in the progressive phase of bleaching, is between that of bleached corals of Yamano et al. (2002) and that of healthy corals (Fig. 4). At sites B3, B4 and B5, whose depth is assumed to be around 1–2 m, a lower DN values were also recorded in 1998 by band 3, whereas no decrease in band 3 values was found at sites B1 and B2. The shallow water depth allowed band 3 to detect the 1998 bleaching event, which agrees well with the results of the radiative transfer simulation (Fig. 5).

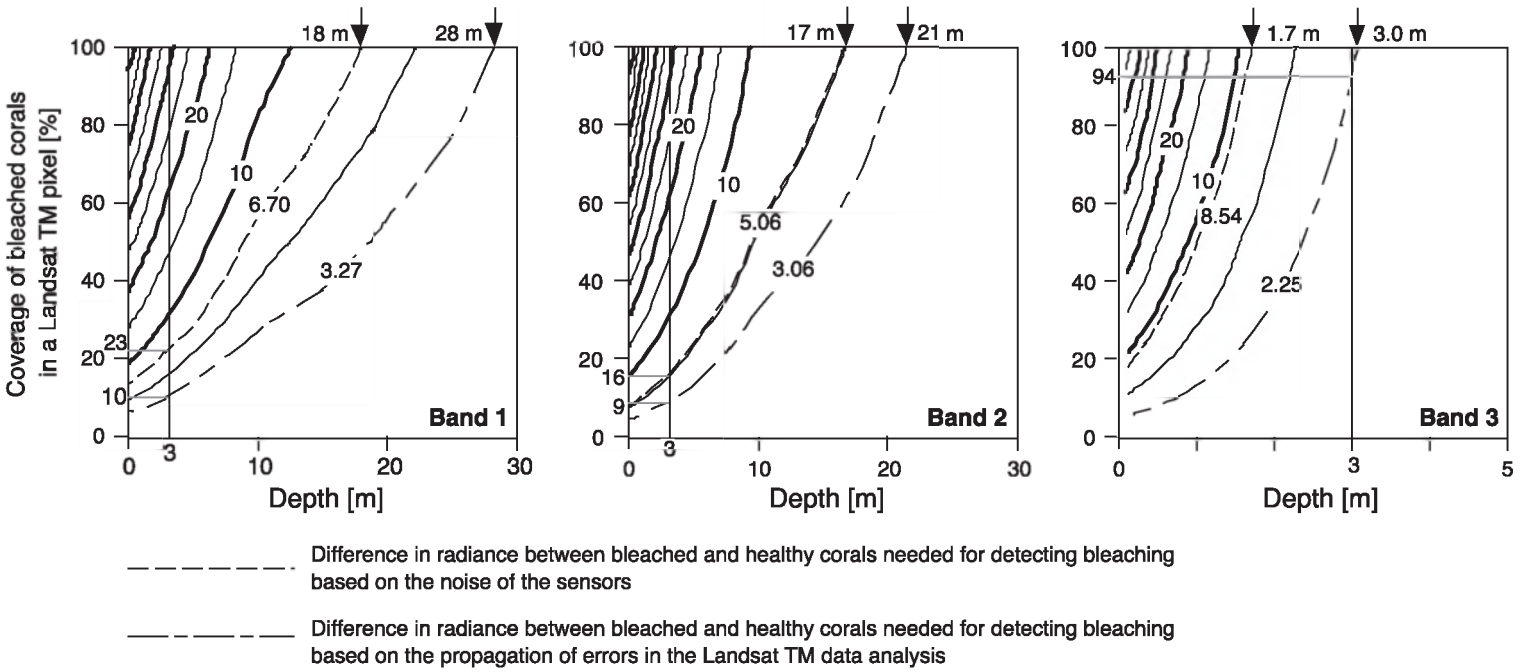

Fig. 5. Contours of calculated differences in radiance values for each Landsat TM band between bleached and healthy corals as a function of water depth and percent cover of bleached corals in a Landsat TM pixel. Vertical lines indicate the maximum depth of coral reef flats (3 m). Percentages show the minimum percent cover of bleached corals in a pixel detectable by Landsat TM, based both on the noise of the sensors only and on the propagation of errors in the Landsat TM data analysis (see text).

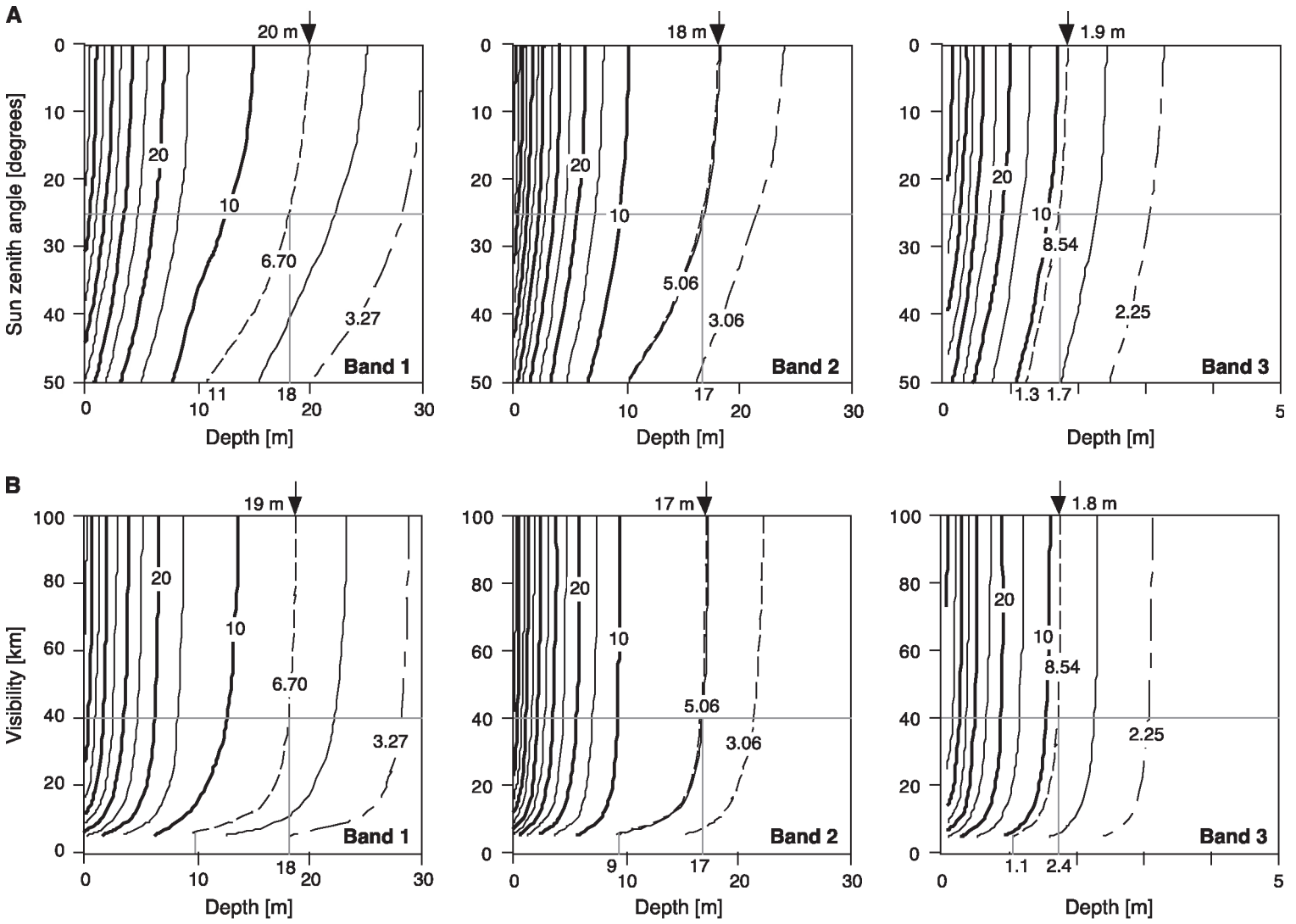

Fig. 6. Contours of calculated differences in radiance values for each Landsat TM band between bleached and healthy corals as a function of water depth and (A) solar zenith angle, (B) visibility, and (C) Chl *a* concentration. Horizontal dotted lines indicates the condition of Ishigaki Island, and vertical dotted lines show the detectable depth at Ishigaki Island, based on the propagation of errors in the Landsat TM data analysis.

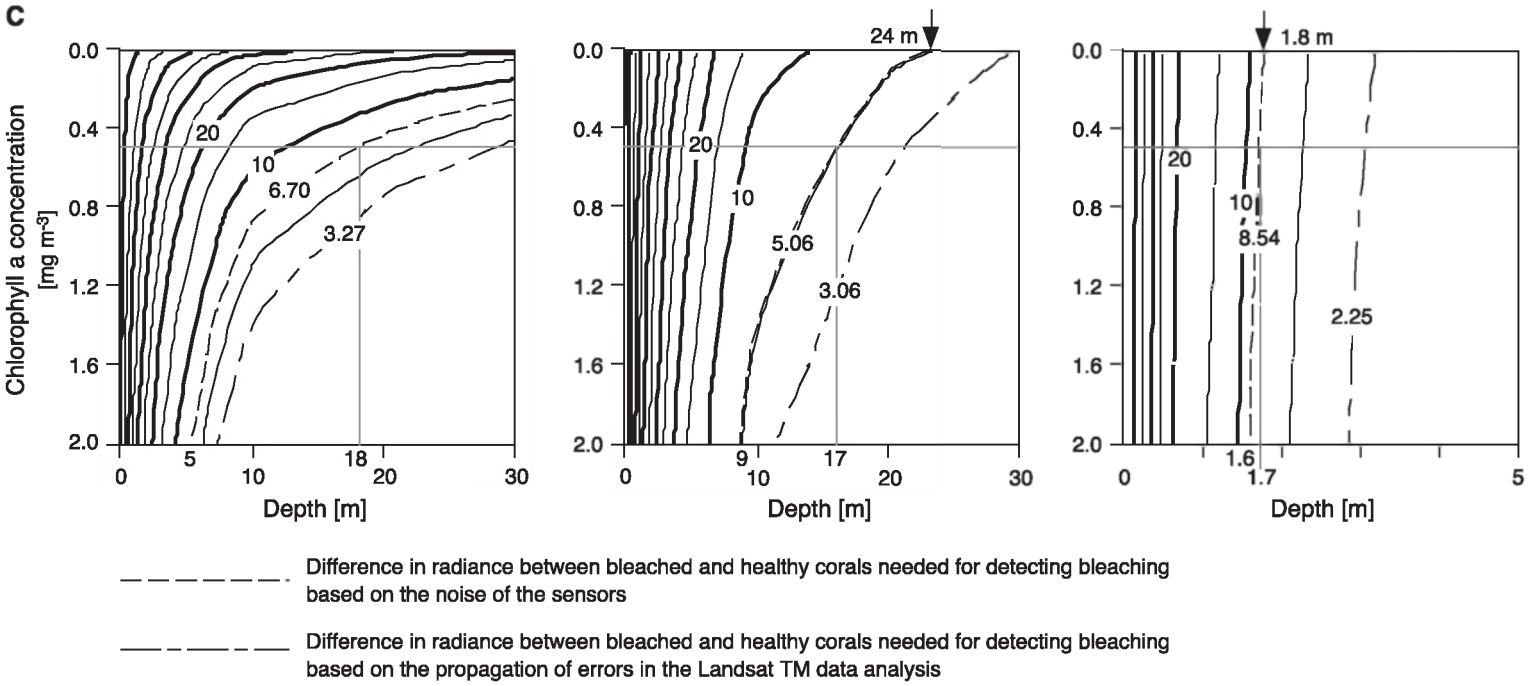

Fig. 6. (*continued*).

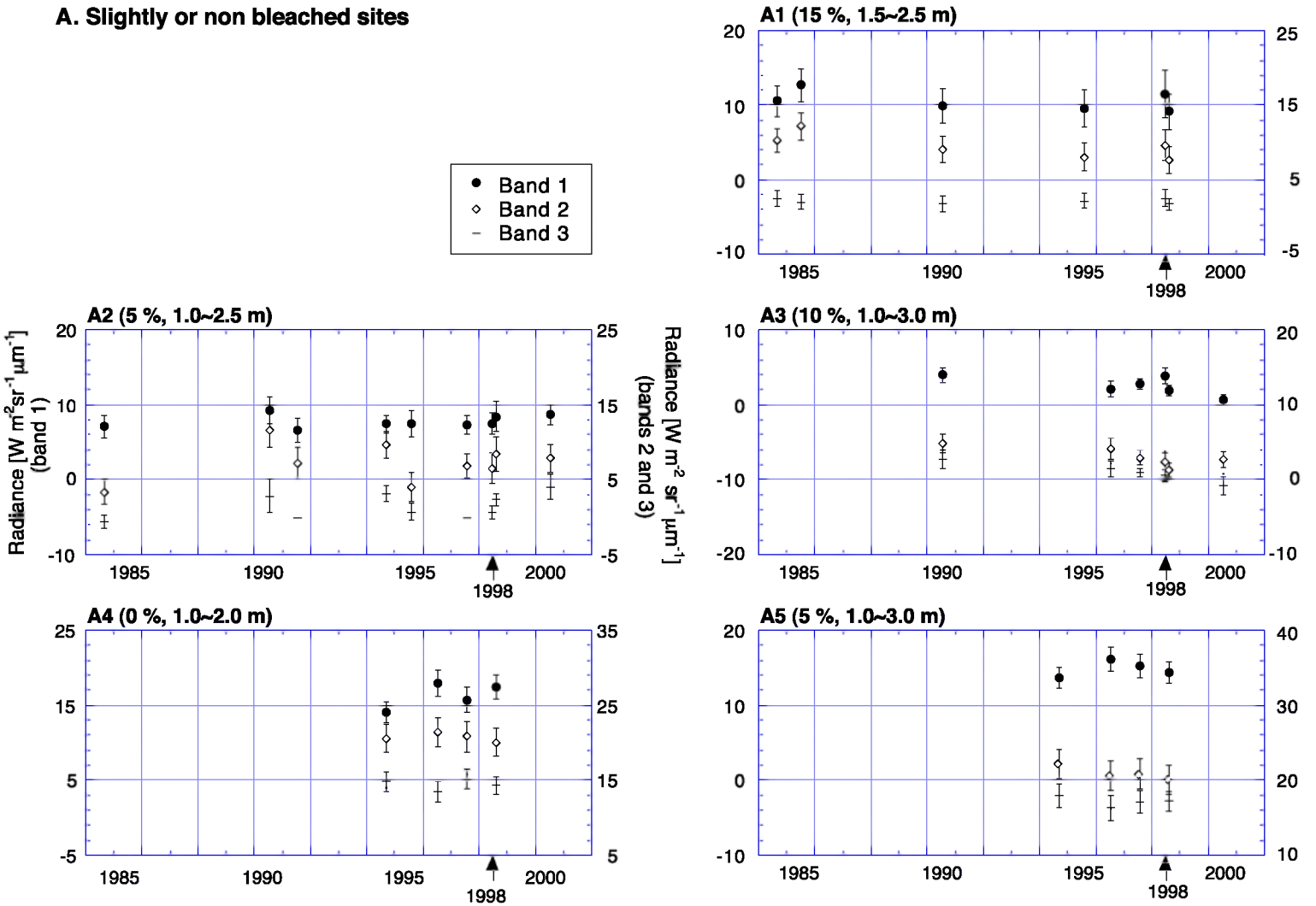

Fig. 7. Temporal changes in the difference of radiance from sand and from corals of Landsat TM bands 1–3 at (A) slightly or non-bleached sites and (B) severely bleached sites. Bars show errors ($\pm 1\sigma$). Percent coverage of bleached corals and water depths at the site are indicated in parentheses.

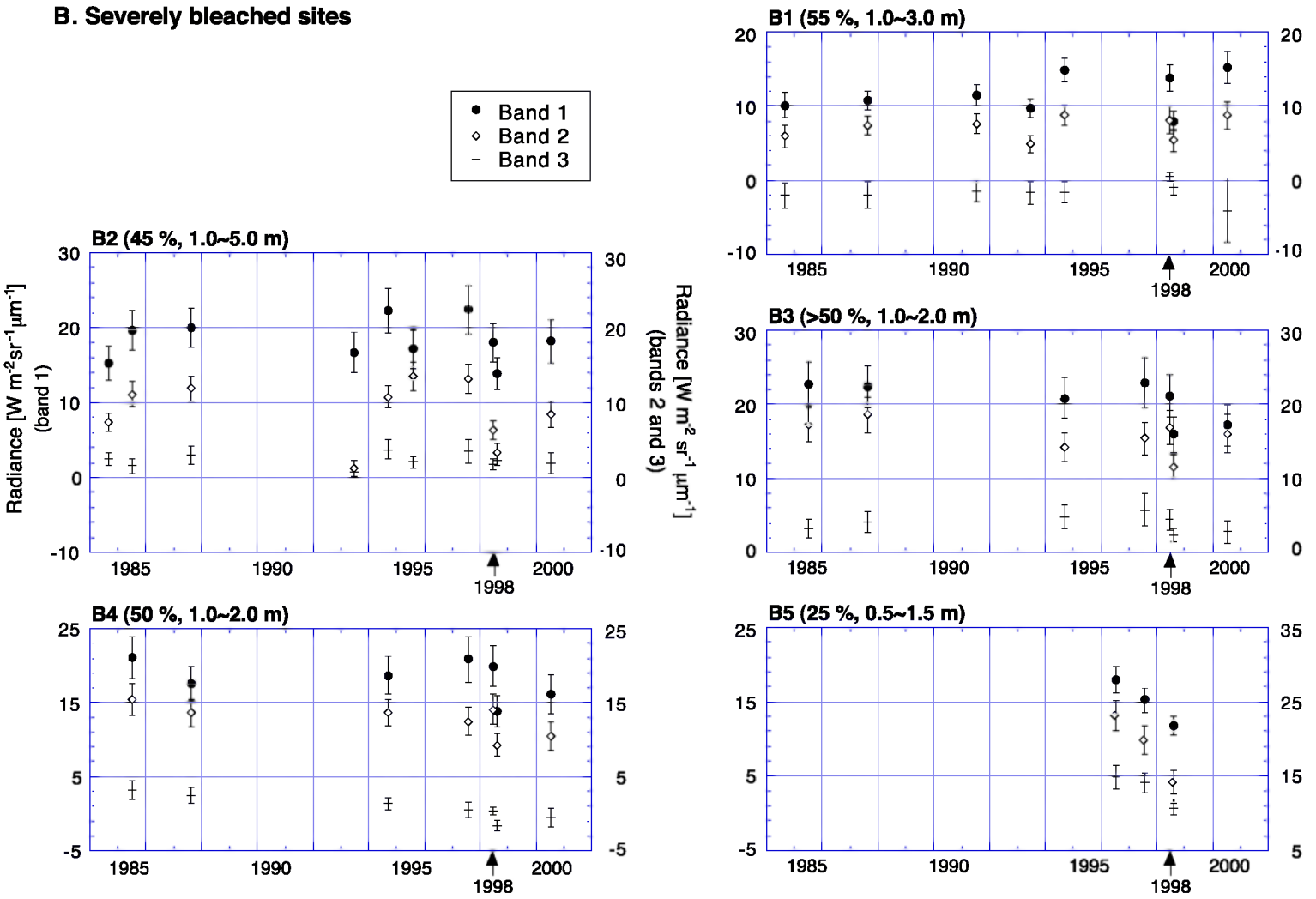

Fig. 7. (*continued*).

The feasibility of Landsat TM for detecting dead corals due to bleaching can also be discussed using Fig. 7B. The detection of coral moralities depends on type of corals and mode of dead corals (Andréfouët et al., 2001), who showed that the shift from brown-type corals to dead coral rubble that was not colonized by macroalgae was potentially detectable. Reflectance of dead coral rubble on Urasaki Reef showed higher values than that of healthy corals (Yamano et al., 2002), which is also shown by Clark et al. (2000) that on a French Polynesian reef where high grazing pressure on macroalgae was observed, corals that had been dead for more than 6 months had higher reflectance values than both living corals and recently dead corals. At sites B2, B3, and B4, where brown *Montipora* corals were initially dominated (Table 1), the small values for July 2000 could be a result of the eventual death of corals, while at site B1, where blue *Acropora* corals were dominated, the value for July 2000 is the same as that before bleaching (Fig. 7B). Thus, as suggested by Andréfouët et al. (2001) for Landsat ETM+, Landsat TM could potentially monitor not only bleaching events, but also the mortality of corals following such events, if the dead corals were initially brown corals and are not then colonized by macroalgae.

Small difference values in some bands at sites B1 and B2 were also observed for 1993 (Fig. 6B). The 1993 bleaching (Fujioka, 1999) could also be detected in this study. The difference values at site B2 for 1984 are also small (Fig. 7B), suggesting that bleaching also took place in 1984. It should be noted that severe typhoons can topple branching coral patches established on sand substrates (Lirman & Fong, 1997; Yamano et al., 2000), which could produce the low values of Fig. 6B. The potential effect of typhoons is observed at slightly or non-bleached sites (in 1984 and 1995 at A2, in 1994 at A4, Fig. 7A). No severe typhoons struck Ishigaki Island in 1997 and 1998, however, and the significant decrease in radiance difference at severely bleached sites in summer 1998 was almost certainly due to the severe bleaching event.

The area that might have been affected by coral bleaching in 1998 is shown in Fig. 8. At Tamatorizaki Reef, no potentially bleached area was identified in areas with high initial coral coverage, which concurs with previous reports (Environment Agency, 1999). At Urasaki Reef, the area of possible coral bleaching in areas with high initial coral coverage is much larger. Some points at the edge of a coral patch might have been bleached, and coral cover increased at some points. This is likely due to spatial misregistration causing contamination of adjacent pixels that consist of sand. Another problem is that some points in a sparsely coral-covered area were identified as potentially bleached. At Urasaki Reef, in addition to coral bleaching, algae on reef areas showed significant decreases. High SST might also affect the growth of algae on coral reefs. This decrease in algae might explain the appearance of potentially bleached areas in otherwise sparsely coral-covered areas.

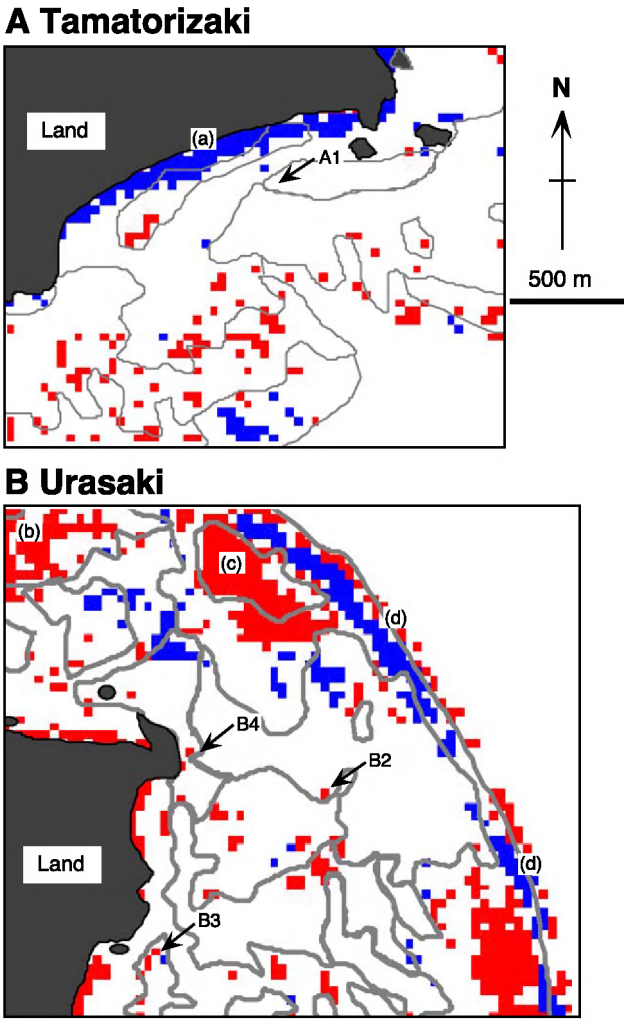

Fig. 8. Potential area of coral reef bleaching in 1998 extracted using the difference of radiance from sand and from corals between August 1995 and August 1998 (A; Tamatorizaki Reef) and between July 1997 and August 1998 (B; Urasaki Reef). Bottom types are as in Fig. 2. Points for temporal change analysis of radiance values (Fig. 2) are indicated by arrows. Blue and red points indicate increase and decrease in radiance values, respectively. Blue points on Tamatorizaki Reef (a) are likely the result of aerial exposure of shallow areas in 1997 due to low water levels (Table 3). Red points on Urasaki Reef (b) are likely because of clouds (Fig. 1). Red points in an area of seaweed (c) reflect the decrease in seaweed in 1998. Blue and red points (d) should be caused by breaking waves at the reef edge.

3.3. Detection limits of coral reef bleaching by satellite remote sensing

From the radiative transfer simulation presented, a bleaching event that produces more than 23% bleached coral cover on reef flats can be detected using Landsat TM bands 1 and 2. From the actual satellite data analysis, a severe bleaching event that produced a 25–55% cover of bleached corals on a reef flat was detected, but slight bleaching resulting in 15% bleached coral cover on a reef flat was not detected. The simulation and data analysis agree well with each other, and identify reliable limits for satellite

remote sensing for detecting coral reef bleaching. In order to detect a bleaching event using Landsat TM, it is necessary to assume bleached coral coverage on a shallow (<3 m depth) reef flat to be at least 23% (210 m^2) throughout a pixel of 900 m^2, because the spatial resolution of Landsat TM is 30 m.

Our results serve as general guidelines for detecting coral reef bleaching using Landsat, and Fig. 6 would be a promising approach to examine the feasibility of satellite remote sensing for detecting coral reef bleaching in general. Because coral reefs are established in a low latitude area where solar zenith angle in summer is less than 25°, the effect of solar zenith angle should be small (Fig. 6A), and the likelihood of detecting coral bleaching will be almost identical to that at Ishigaki Island. For aerosol (visibility) (Fig. 6B), in tropical coral reef areas, Pacific oceanic islands have high visibility (Smirnov et al., 2002; Yu et al., 2003), and thus our results at Ishigaki Island can be applied without consideration of aerosol. However, the visibility often shows less than 25 km in Caribbean Sea, Indian Ocean and Southeast Asia, and this low visibility has been attributed to dust, pollutant or forest fires (Kobayashi et al., in press; Yu et al., 2003). Low (<25 km) visibility would decrease significantly the maximum detectable depth as indicated in Fig. 6B, and thus the visibility is a factor that should be considered in detecting bleaching. The likelihood of bleaching detection is most sensitive to Chl *a* (Fig. 6C). Using band 1, however, the likelihood of the detection is expected to be greater than that in Ishigaki Island, because many coral reefs have Chl *a* concentration smaller than 0.5 mg m^{-3} (e.g., 0.3 – 0.5 mg m^{-3} in the Great Barrier Reef of Australia, Brodie et al., 1997; 0.03–0.43 mg m^{-3} in Tuamotu atoll lagoons, Charpy et al., 1997). In high (>0.5 mg m^{-3}) and variable Chl *a* concentrations, use of band 2 would result in reliable detection, as the maximum depth was not affected significantly in band 2 (Fig. 6C).

Some limiting factors for the bleaching detection can be presented. The reflectance data used for bleached corals are for almost totally bleached coral; patchy bleaching is to be expected in a pixel of 900 m^2, however, which reduces the reliability of satellite remote sensing. Spatial misregistration resulted in a high degree of uncertainty in the detection of changes at the edges of coral patches. Therefore, even after removing and normalizing atmospheric effects that are commonly problematic, satellite remote sensing is limited in its ability to detect coral bleaching, mainly because of the low (~30 m) spatial resolution, which enhances the possibility of misidentification of objects and misrepresentation of partly bleached coral, and also exaggerates the effect of spatial misregistration. Detection of coral reef bleaching by Landsat TM is limited to sites that have particularly high coral cover over large areas (Fig. 8). Typhoons that topple branching corals should be carefully examined, because sand has a higher reflectance than corals and can be easily interpreted as bleached corals in the present analysis.

These limitations, however, can be overcome using high spatial resolution sensors. Because bleached coral has a higher reflectance than healthy coral in the visible wavelength range (Fig. 4), the limiting factor is not spectral resolution but spatial resolution. Given the heterogeneous nature of coral reefs, higher spatial resolution should result in better detection of bleaching. The thematic accuracy increased using IKONOS whose spatial resolution is 4 m (Andréfouët et al., 2003; Mumby & Edwards, 2002), which would contribute to detailed coral mapping. Furthermore, because sand often occurs with broader/low frequency spatial distribution, some spatial variability analysis would help minimize the problem caused by typhoon toppling. In addition to high spatial resolution, a shorter recurrence interval for the satellites would be preferable than afforded by Landsat, in order to monitor the progress of bleaching events. Satellite remote sensing of coral reef bleaching should be encouraged in the future, as advanced satellite sensors with high spatial resolution (e.g., IKONOS, QuickBird, ALOS) are developed and deployed, and they are contributing to bleaching detection (Elvidge et al., in press).

Acknowledgements

We are grateful to Osamu Abe, Yohei Matsui, Saki Harii and Akio Obata for their field assistance at Ishigaki Island. Michio Hidaka and Yoshimitsu Kunii contributed to measuring coral reflectance spectra. Midori Togashi and Masayasu Maki helped us in georeferencing the Landsat TM images. Minoru Yoshida provided information on survey method for monitoring coral coverage. Data on Chl *a* were provided through the courtesy of Hiroshi Hata and Hajime Kayanne. Hideki Kobayashi provided fruitful discussion on aerosol and visibility. Finally, we would like to sincerely thank anonymous reviewers, whose comments and suggestions significantly improved the manuscript. This paper is a contribution to the joint research project with NASDA (National Space Development Agency of Japan) entitled "Use of ALOS data for monitoring coral reef bleaching."

References

Ahmad, W., & Neil, D. T. (1994). An evaluation of Landsat Thematic Mapper (TM) digital data for discriminating coral reef zonation: Heron Reef (GBR). *International Journal of Remote Sensing*, *15*, 2583–2597.

Akatsuka, I. (2001). Seasonal and yearly changes of seaweed vegetation in Isigaki-zima Island and Iriomote-zima Island of Yaeyama Islands. WWF Japan-Funded Research Report 2000 (in Japanese).

Andréfouët, S., Berklemans, R., Odrizola, L., Done, T., Oliver, J., & Muller-Karger, F. (2002). Choosing the appropriate spatial resolution for monitoring coral bleaching events using remote sensing. *Coral Reefs*, *21*, 147–154.

Andréfouët, S., Kramer, P., Torres-Pulliza, D., Joyce, K. E., Hochberg, E. J., Garza-Perez, R., Mumby, P. J., Riegl, B., Yamano, H., White, W. H., Zubia, M., Brock, J. C., Phinn, S. R., Naseer, A., Hatcher, B. G., &

Muller-Karger, F. (2003). Multi-site evaluation of IKONOS data for classification of tropical coral reef environments. *Remote Sensing of Environment*, *88*, 128–143.

Andréfouët, S., Muller-Karger, F. E., Hochberg, E. J., Hu, C., & Carder, K. L. (2001). Change detection in shallow coral reef environments using Landsat 7 ETM+ data. *Remote Sensing of Environment*, *78*, 150–162.

Brodie, J. E., Furnas, M. J., Steven, A. D. L., Trott, L. A., Pantus, F., & Wright, M. (1997). Monitoring chlorophyll in the Great Barrier Reef lagoon: Trends and variability. *Proceedings of the 8th International Coral Reef Symposium, vol. 1* (pp. 797–802), Balboa, Panama.

Brown, B. E. (1997). Coral bleaching: Causes and consequences. *Coral Reefs*, *16*, S129–S138 (Suppl.).

Bukata, R. P., Jerome, J. H., Kondratyev, K. Y., & Pozdnyakov, D. V. (1995). *Optical properties and remote sensing of inland and coastal waters*. Florida: CRC Press.

Charpy, L., Dufour, P., & Garcia, N. (1997). Particulate organic matter in sixteen Tuamotu atoll lagoons (French Polynesia). *Marine Ecology Progress Series*, *151*, 55–65.

Clark, C. D., Mumby, P. J., Chisholm, J. R. M., Jaubert, J., & Andrefouet, S. (2000). Spectral discrimination of coral mortality states following a severe bleaching event. *International Journal of Remote Sensing*, *21*, 2321–2327.

Elvidge, C. D., Dietz, R. J. B., Berklemans, R., Andréfouët, S., Skirving, W., Strong, A. E., & Tuttle, B. T. (in press). Satellite observation of Keppel Islands (Great Barrier Reef) 2002 coral bleaching using IKONOS data. Coral Reefs.

Environment Agency (1996). *Marine biotic survey (1989–1992) in the 4th national survey on the natural environment: 1/10,000 distribution map of coral reefs*. Tokyo: Environment Agency (in Japanese).

Environment Agency (1999). *Report of coral reef monitoring around the Ishigaki Island (Year of Heisei 10)*. Tokyo: Environment Agency (in Japanese).

Environment Agency (2000a). *Report of coral reef monitoring around the Ishigaki Island (Year of Heisei 11)*. Tokyo: Environment Agency (in Japanese).

Environment Agency (2000b). *Report of coral reef monitoring around the Ishigaki Island (Year of Heisei 12)*. Tokyo: Environment Agency (in Japanese).

Fujioka, Y. (1999). Mass destruction of the hermatypic corals during a bleaching event in Ishigaki Island, southwestern Japan. *Galaxea, JCRS*, *1*, 41–50.

Glynn, P. W. (1993). Coral reef bleaching: Ecological perspectives. *Coral Reefs*, *12*, 1–17.

Goreau, T. J., & Hayes, R. L. (1994). Coral bleaching and ocean "hot spots". *Ambio*, *23*, 176–180.

Haltrin, V. I. (1999). Chlorophyll-based model of seawater optical properties. *Applied Optics*, *38*, 6826–6832.

Hasegawa, H., Ichikawa, K., Kobayashi, M., Kobayashi, T., Hoshino, M., & Mezaki, S. (1999). The mass-bleaching of coral reefs in the Ishigaki Lagoon, 1998. *Galaxea, JCRS*, *1*, 31–39 (in Japanase with English abstract).

Hochberg, E. J., & Atkinson, M. J. (2000). Spectral discrimination of coral reef benthic communities. *Coral Reefs*, *19*, 164–171.

Hochberg, E. J., Atkinson, M. J., & Andréfouët, S. (2003). Spectral reflectance of coral reef bottom-types worldwide and implications for coral reef remote sensing. *Remote Sensing of Environment*, *85*, 159–173.

Hoegh-Guldberg, O. (1999). Climate change, coral bleaching and the future of the world's coral reefs. *Marine and Freshwater Research*, *50*, 839–866.

Holden, H., & LeDrew, E. (1998). Spectral discrimination of healthy and non-healthy corals based on cluster analysis, principal components analysis, and derivative spectroscopy. *Remote Sensing of Environment*, *65*, *217–224*.

Holden, H., & LeDrew, E. (1999). Hyperspectral identification of coral reef features. *International Journal of Remote Sensing*, *20*, 2545–2563.

Kayanne, H., Harii, S., Ide, Y., & Akimoto, F. (2002). Recovery of coral populations after the 1998 bleaching on Shiraho Reef, in the southern Ryukyus, NW Pacific. *Marine Ecology Progress Series*, *239*, 93–103.

Kirk, J. T. O. (1994). *Light and photosynthesis in aquatic ecosystems*. New York: Cambridge University Press.

Kobayashi, H., Matsunaga, T., Hoyano, A., Aoki, M., Komori, D., & Boonyawat, S. (in press). Satellite estimation of photosynthetically active radiation in Southeast Asia: Impacts of smoke and cloud cover. *Journal of Geophysical Research*.

Lirman, D., & Biber, P. (2000). Seasonal dynamics of macroalgal communities of the northern Florida reef tract. *Botanica Marina*, *43*, 305–314.

Lirman, D., & Fong, P. (1997). Patterns of damage to the branching coral *Acropora palmata* following Hurricane Andrew: Damage and survivorship of hurricane-generated asexual recruits. *Journal of Coastal Research*, *13*, 67–72.

Lubin, D., Li, W., Dustan, P., Mazel, C. H., & Stamnes, K. (2001). Spectral signatures of coral reefs: Features from space. *Remote Sensing of Environment*, *75*, 127–137.

Lyzenga, D. R. (1978). Passive remote sensing techniques for mapping water depth and bottom features. *Applied Optics*, *17*, 379–383.

Lyzenga, D. R. (1981). Remote sensing of bottom reflectance and water attenuation parameters in shallow water using aircraft and Landsat data. *International Journal of Remote Sensing*, *2*, 71–82.

Matsunaga, T., Hoyano, A., & Mizukami, Y. (2000). Monitoring of coral reefs on Ishigaki Island in Japan using multitemporal remote sensing data. *Proceedings of SPIE, vol. 4154* (pp. 212–222), Sendai, Japan.

Mobley, C. D. (1994). *Light and water: Radiative transfer in natural waters*. London: Academic Press.

Mumby, P. J., Clark, C. D., Green, E. P., & Edwards, A. J. (1998a). Benefits of water column correction and contextual editing for mapping coral reefs. *International Journal of Remote Sensing*, *19*, 203–210.

Mumby, P. J., & Edwards, A. J. (2002). Mapping marine environments with IKONOS imagery: Enhanced spatial resolution can deliver greater thematic accuracy. *Remote Sensing of Environment*, *82*, *248–257*.

Mumby, P. J., Green, E. P., Clark, C. D., & Edwards, A. J. (1998b). Digital analysis of multispectral airborne imagery of coral reefs. *Coral Reefs*, *17*, 59–69.

Myers, M. R., Hardy, J. T., Mazel, C. H., & Dustan, P. (1999). Optical spectra and pigmentation of Caribbean reef corals and macroalgae. *Coral Reefs*, *18*, 179–186.

Smirnov, A., Holben, B. N., Kaufman, Y. J., Dubonik, O., Eck, T. F., Slutsker, I., Pietras, C., & Halthore, R. N. (2002). Optical properties of atmospheric aerosol in maritime environments. *Journal of the Atmospheric Sciences*, *59*, 501–523.

Stow, D. A. (1999). Reducing the effects of misregistration on pixel-level change detection. *International Journal of Remote Sensing*, *20*, 2477–2483.

Strong, A. E., Barrientos, C. S., Duba, C., & Sapper, J. (1997). Improved satellite techniques for monitoring coral reef bleaching. *Proceedings of the 8th International Coral Reef Symposium, vol. 2* (pp. 1495–1498), Balboa, Panama.

Strong, A. E., Liu, G., Kimura, T., Yamano, H., Tsuchiya, M., Kakuma, S., & van Woesik, R. (2002). Detecting and monitoring 2001 coral reef bleaching events in Ryukyu Islands, Japan using satellite bleaching HotSpot remote sensing technique. *Proceedings of International Geoscience and Remote Sensing Symposium 2002, vol. I* (pp. 237–239), Toronto, Canada.

Thome, K., Markham, B., Barker, J., Slater, P., & Biggar, S. (1997). Radiometric calibration of Landsat. *Photogrammetric Engineering and Remote Sensing*, *63*, 853–858.

Vermote, E. F., Tanré, D., Deuzé, J. L., Herman, M., & Morcrette, J. -J. (1997). Second simulation of the satellite signal in the solar spectrum, 6S: An overview. *IEEE Transactions on Geoscience and Remote Sensing*, *35*, 675–686.

Wilkinson, C. R. (2000). *Status of coral reefs of the world: 2000*. Queensland: Australian Institute of Marine Science.

Yamano, H., Kayanne, H., Yonekura, N., & Kudo, K. (2000). 21-year changes of backreef coral distribution: Causes and significance. *Journal of Coastal Research*, *16*, 99–110.

Yamano, H., & Tamura, M. (2001). Use of Landsat TM data and radiative transfer models for monitoring coral reef bleaching. *Proceedings of International Geoscience and Remote Sensing Symposium 2001, vol. V* (pp. 2199–2201), Sydney, Australia.

Yamano, H., & Tamura, M. (2002). Can satellite sensors detect coral reef bleaching? A feasibility study using radiative transfer models in air and water. *Proceedings of the 9th international coral reef symposium* (pp. 1025–1030), Bali, Indonesia.

Yamano, H., Tamura, M., Kunii, Y., & Hidaka, M. (2002). Hyperspectral remote sensing and radiative transfer simulation as a tool for monitoring coral reef health. *Marine Technology Society Journal*, *36*, 4–13.

Yamano, H., Tamura, M., Kunii, Y., & Hidaka, M. (2003). Spectral reflectance as a potential tool for detecting stressed corals. *Galaxea, JCRS*, *5*, 1–10.

Yu, H., Dickinson, R. E., Chin, M., Kaufman, Y. J., Holben, B. N., Geogdzhayev, I. V., & Mischenko, M. I. (2003). Annual cycle of global distributions of aerosol optical depth from integration of MODIS retrievals and GOCART model simulations. *Journal of Geophysical Research*, *108*, 4128.